

Your Interlibrary Loan request has been sent by email in a PDF format.

If this PDF arrives with an incorrect OCLC status, please contact lending located below.

Concerning Copyright Restrictions

The copyright law of the United States (Title 17, United States Code) governs the making of photocopies or other reproductions of copyrighted materials. Under certain conditions specified in the law, libraries and archives are authorized to furnish a photocopy or other reproduction. One of these specified conditions is that the photocopy or reproduction is not to be "used for any purpose other than private study, scholarship, or research". If a user makes a request for, or later uses, a photocopy or reproduction for purpose in excess of "fair use", that user may be liable for copyright infringement. This institution reserves the right to refuse to accept a copying order if, in its judgment, fulfillment of the order would involve violation of copyright law.

Interlibrary Loan Services: We Search the World for You...and Deliver!

Interlibrary Loan Services
The Florida State University
711 West Madison Street
Tallahassee, Florida 32306-1005

Lending the FSU Collection: 850.644.4171
James Elliott- ILL- lend@reserves.lib.fsu.edu

Borrowing for the FSU Community: 850.644.4466
Alicia Brown- ill@reserves.lib.fsu.edu

Odyssey: 128.186.59.120 Ariel: 146.201.65.22
Fax: 850.644.3329



Single-cylinder engine evaluation of a multi-component Diesel surrogate fuel at partially-premixed and low-temperature combustion modes

Patrick G. Szymkowicz^{a,*}, Jesús Benajes^b

^a Diesel Engine Systems Group, Propulsion Systems Research Lab, GM Global Research & Development, 800 North Glenwood Ave., Pontiac, MI 48340-2925, USA

^b CMT-Motores Térmicos, Universitat Politècnica de València, Camino de Vera s/n, 46022 Valencia, Spain

ARTICLE INFO

Keywords:

Diesel fuel
Surrogate fuel
Diesel combustion
Partially-premixed combustion
Low-temperature combustion
Fuel properties
Cetane number
Threshold soot index
Exhaust emissions
Soot
Exhaust particles

ABSTRACT

To investigate and develop efficient and clean combustion systems, advanced CFD modeling tools need accurate kinetic models capable of predicting the chemical and physical processes that take place in the combustion chamber during and after fuel injection and air mixing. Given the complex composition of market Diesel fuels, simpler surrogate fuels composed of a limited number of pure substances are used to model the physical, chemical, and combustion properties of Diesel fuel. The surrogates must closely reproduce the market Diesel fuel properties and duplicate the real-world engine combustion and emissions behavior. Previous work created a multi-component surrogate fuel that consisted of normal-hexadecane/2,2,4,4,6,8,8-heptamethylnonane/decahydronaphthalene/1-methylnaphthalene. The surrogate fuel properties closely matched the market Diesel fuel. The surrogate fuel was then evaluated under conventional Diesel engine combustion conditions and obtained excellent results replicating the real-world combustion and emissions of the market Diesel fuel. In this work, the surrogate fuel was investigated using a contemporary Diesel engine, operating at a low-load where partially-premixed and low temperature combustion conditions were achieved. For comparison and validation, the original market Diesel fuel was also tested under the same operating conditions. The experimental results from EGR and combustion phasing sweeps under partially-premixed and low temperature combustion showed the surrogate fuel closely duplicated the ignition delay, low temperature and high temperature heat release of the market Diesel fuel. The exhaust CO, NOx and HC emissions along with the particle size distributions were also closely matched. This investigation demonstrates that the four-component surrogate accurately represents the market Diesel fuel under low load, premixed and low temperature combustion regimes. Therefore, the surrogate fuel formulation should be suitable for continued work such as kinetic mechanism development, 3-dimensional spray and combustion simulation, and further exploratory research under premixed and low temperature combustion conditions.

1. Introduction

Despite the current criticism of Diesel-engine powered cars, Diesel engines are still a key pathway towards mitigating the trend of growing CO₂ emissions from transportation. For example, in the sector of passenger cars and light-duty vehicles, Diesel engines are able to generate up to 20% less CO₂ than gasoline equivalents [1]. In addition to this advantage, modern Diesel engines, coupled with a matched after-treatment system, emit very low levels of pollutants at the tailpipe. However, the required aftertreatment devices add significant complexity and increase the vehicle costs, in terms of purchase, operation and maintenance.

Hence, achieving reduced engine-out emissions is a very interesting resource for alleviating the complexity and cost of the aftertreatment

systems [2]. This objective can be attained by putting internal measures in operation that produce a cleaner combustion process, sometimes different from the conventional Diesel combustion, like the partially premixed compression-ignition (PPCI) and low-temperature combustion (LTC), able to reduce engine-out NOx and soot emissions [3–5].

In any case, to efficiently develop advanced Diesel combustion systems, CFD modeling tools are usually required, and in particular, practical spray and combustion models that quantitatively predict engine combustion and emissions. Specifically, accurate kinetic models are necessary to predict the chemical processes that take place during and after injection and air mixing: low temperature reactions, auto ignition, heat release, exhaust emissions, and soot.

Given the complex composition of market Diesel fuels, simpler surrogate fuels composed by a limited number of pure substances are

* Corresponding author.

Nomenclature	
A/F	Air-to-fuel ratio
ASTM	American Society for Testing and Materials
aTDC	After Top Dead Center
CA50	Crank-angle of 50% mass burned
CAD	Crank-Angle Degrees
CMD	Count Median Diameter
CN	Cetane Number
CO	Carbon monoxide
CO ₂	Carbon dioxide
D _p	Particle diameter
EGR	Exhaust Gas Recirculation
EI	Emission Index
FSN	Filter Smoke Number
HC	Hydrocarbons
HRR	Heat Release Rate
HTHR	High Temperature Heat Release
IMEP	Indicated Mean Effective Pressure
LTC	Low Temperature Combustion
LTHR	Low Temperature Heat Release
N	Number of particles
N/cc	Particle number concentration
NOx	Nitrous Oxides
O ₂	Oxygen
PPCI	Partially-Premixed Compression Ignition
SOE	Start of Energizing of fuel injector
SOI	Start of Injection
TSI	Threshold Soot Index

used to model the physical, chemical and combustion properties of Diesel fuel [6–9]. Assuming that detailed kinetic mechanisms are available for each single component of the surrogate fuel, kinetic mechanisms can be assembled and validated for the complete surrogate fuel. The temperature dependent properties of the surrogate are often modeled using correlations developed by the Design Institute for Physical Properties [10]. Applying this procedure, it is possible to formulate fully-representative surrogate fuels that accurately replicate the physical, chemical and combustion properties of the market Diesel fuel [11,12].

The simpler surrogates are those based on a single substance, like n-heptane to model combustion kinetics [13–15] and n-dodecane to model fuel physical properties [16,17]. Despite having significantly expanded the fundamental understanding of Diesel combustion, single component surrogates can only mimic a limited number of fuel properties, and in general, multi-component surrogate fuels are required to fully represent the properties of a market Diesel fuel [8,11,12].

A step further, especially to better mimic the sooty tendency of Diesel fuel, are the binary surrogates that combine a normal-alkane with an aromatic species, for example n-decane and 1-methyl-naphthalene, n-heptane and toluene or n-dodecane and m-xylene [18].

Increasing the number of components in the surrogate would give more flexibility in mimicking the Diesel fuel properties and also in reproducing the spray atomization, air-fuel mixing, ignition, combustion, and pollutant formation. Exceptional progress has been made in this sense, by the increasing availability of kinetic mechanisms for numerous hydrocarbon species constituents of the surrogate [8,19,20]. For example, Johnson et al., investigated the auto ignition properties of jet fuels and simple surrogate fuels using a Cooperative Fuel Research (CFR) Diesel engine [21]. Poon et al. developed a four-component Diesel surrogate that consisted of n-hexadecane, heptamethylnonane, cyclohexane and toluene [22,23]. Mueller et al., formulated a set of multi-component surrogate fuels ranging from four components up to nine components. The four-component surrogate consisted of n-hexadecane, heptamethylnonane, trans-decalin and 1-methylnaphthalene [11].

The authors of the present study developed a Diesel Surrogate Fuel Library that consisted of 18 surrogate fuels developed adhering to a set of practical requirements to enable the immediate application of the surrogates [24]. The surrogate fuel formulations and predicted properties were validated by blending a subset of surrogate fuels with cetane numbers ranging from 40 to 60 and TSI values spanning from 17 to 48. The properties of the surrogates were measured under ASTM protocols. Excellent agreement between predicted and measured properties were obtained [24]. In addition, the properties of the fuels with the Surrogate Fuel Library were measured and found to be within the range of properties measured from a set of five market Diesel fuels. Within the library, a surrogate was developed to replicate the properties of a

baseline market Diesel fuel with a cetane number of 50 and a TSI value of 31. The surrogate and market Diesel fuel exhibited very similar properties. However, the question of whether both fuels would produce similar combustion and emission results under real-world engine operating conditions called for verification.

In a first instance, both the market Diesel fuel and the surrogate were evaluated by engine tests conducted at a medium load engine operating point, at which the Diesel combustion demonstrated low-temperature heat release, premixed and diffusion combustion regimes [25]. The fuels were tested over broad EGR and combustion phasing sweeps. The test results showed the engine combustion behaviors of the market Diesel fuel were closely matched by the surrogate. The exhaust CO, HC, NOx, smoke and particle size distributions were also in good agreement.

2. Motivation and objectives

PPCI combustion avoids the soot formation by achieving fuel-air mixtures with local equivalence ratios that are generally less than 2. This is also known as smoke-free combustion [26]. The diffusion-controlled combustion phase is essentially absent under PPCI conditions, thereby eliminating the primary source of soot formation. However, depending on the engine operating conditions, PPCI combustion can occur at high temperatures that promote the formation of NOx.

LTC avoids the soot and NOx formation regimes by achieving local combustion temperatures that are generally less than 1500 K [4,26]. This is generally accomplished through charge dilution with high EGR levels. In general, LTC also has longer ignition delays with sufficient fuel-air mixing that results in PPCI combustion. Therefore, the diffusion combustion regime is also avoided with LTC.

Researchers have demonstrated the low NOx and low soot advantages of several LTC strategies. However, investigators also recognized the penalties associated with LTC including significantly increased CO and HC emissions due to incomplete combustion [27,28]. More recently, researchers have shown that LTC also affects the nucleation particle emissions [29–31]. Indeed, the combustion and emissions differences between conventional Diesel combustion and LTC are significant.

Given the potential of the alternative combustion strategies like PPCI and LTC, the current work explored the engine combustion and emissions response of the market Diesel fuel and the surrogate in a single-cylinder Diesel engine operating at a very light load and with large EGR rates. Compared to multi-cylinder engine testing, single-cylinder engine tests provided a means for excellent control and reproducibility of the operating conditions [32].

In addition to examining the surrogate fuel, this effort was conducted to assess the hypothesis that closely matching the physical, chemical and combustion properties of a market Diesel fuel can provide

a practical and effective surrogate even though the particular hydrocarbon species that composes the surrogate may be sparsely present, or not present, in the market Diesel fuel.

3. Experimental methodology

3.1. Fuels

Aside from the market Diesel fuel with a cetane number of 50 and a TSI of 31 the tests were carried out with a four-component surrogate fuel developed by the authors that closely matches the physical, chemical and combustion properties of the Diesel fuel [12,24]. The four components included n-hexadecane to represent the n-alkane class, 2,2,4,4,6,8,8-heptamethylnonane to represent the isoalkane class, decahydronaphthalene to represent the cycloalkane class, and the aromatics were represented by 1-methylnaphthalene. The volume fractions for the surrogate components were: n-hexadecane = 0.37, heptamethylnonane = 0.33, decahydronaphthalene = 0.18 and 1-methylnaphthalene = 0.12. Table 1 presents the ASTM measured properties for the market Diesel fuel and the surrogate, which will be named as CN50_TSI31 in this paper. A correlation developed by Riazi and Dauert was used to calculate the average molecular weight of the market Diesel fuel [33]. TSI was determined by the method defined by Calcote and Manos [34]. A lubricity improver was added to the surrogate fuel (100 ppm) to safeguard the proper operation of the fuel injection system.

The surrogate fuel was blended without alkenes. However, test results reported 4.9% v/v alkenes in the surrogate. To investigate the source of alkenes, ASTM results from 5 surrogates with substantial differences in the volume fractions of the components were analyzed. The alkene levels varied from 2 to 5% and did not correlate to any single fuel component. Since the remaining combustion, physical and chemical properties of the 5 surrogates fuel were found to be in close agreement with predicted surrogate fuel properties [12,24], it was concluded the alkenes did not have a measurable effect on the properties of the surrogate fuel.

3.2. Engine and test cell

A single-cylinder research engine was fitted with a production engine combustion system from a 4-cylinder engine. The combustion system included the 4-valve cylinder head, piston, connecting rod, and fuel injection system. The primary engine characteristics are given in Table 2, while a schematic diagram of the engine test facility is shown in Fig. 1.

A Kistler Type 4067C3000S pressure sensor was installed in the high-pressure fuel line, between the rail and the injector. As defined in Fig. 2, an inflection point in the fuel line pressure was used to infer the start of fuel injection (SOI). The injector needle opening delay was calculated from the inferred start of injection and the start of energizing (SOE) from the injector current signal. The injection events were determined with an accuracy of ± 0.2 CAD.

The excessive cost of testing coupled with the availability of the engine dynamometer facilities prevented the required triplicate testing to create confidence intervals. Therefore, several procedures were implemented to ensure the accuracy and correctness of the data. For example, to ensure the accuracy of the emission measurements, the gas analyzers were calibrated prior to each set of sweeps. Precision blended gas mixtures of CO, NO, NO₂, propane, and O₂ (from calibration standard compressed gas bottles) were measured each day and control charted to verify the proper functioning of all the emission analyzers. Engine motoring and firing checkpoints were run twice a day and the data used for quality control charts. Engine blow-by was continuously monitored.

3.2.1. In-cylinder pressure analysis and ignition delay

Engine combustion was measured with a Kistler Type 6125C10 pressure sensor flush-mounted in a glow plug adapter. Instantaneous in-cylinder pressure data were sampled for 150 consecutive engine cycles at a crank-angle resolution of 0.2 degrees. In-cylinder pressure was computed by ensemble-averaging the data of the pressure transducer along the 150 cycles. The high number of cycles and the typical accuracy of the pressure transducer was deemed sufficient for ensuring the desired significance and accuracy. The apparent net heat-release was calculated from the in-cylinder pressure data, as described by Heywood [35] and Gatowski et al. [36] which includes the heat transfer loss to the combustion chamber and cylinder walls. Within this paper, and for brevity, the apparent net heat-release rate is simply referred to as heat-release rate (J/CAD). Ignition delay was defined as the period between the start of fuel injection (as defined in Fig. 2) and the crank angle of 5% mass burned fraction.

The calculation of indicated, net and pumping mean effective pressures (IMEP, NMEP, PMEP) were consistent with methods reported in Heywood [35] and the UPV-CMT analysis code CALMEC from Lapuerta [37] and Payri [38]. A modified Rassweiler-Withrow type heat-release analysis provided combustion burn periods from which combustion phasing parameters such as the crank-angle of 50% mass burned fraction were obtained. Further details are given in the CAS Reference Manual [39].

3.2.2. Air and fuel flow

A critical air flow supply system provided accurately controlled intake air pressure and precise mass flow measurement. The system consisted of six precision nozzles of varying size calibrated as sonic flow nozzles.

An AVL P404 Fuel Measurement Cart supplied low pressure fuel to the high-pressure fuel pump and provided fuel conditioning, density and mass flow measurements. Due to the very low flow rates typical of single-cylinder engines at light loads, a special low-flow fuel meter with a high-precision calibration was installed in the cart.

3.2.3. Pressure and temperature

Static pressures were measured with transducers appropriately sized for the required pressure ranges. High-speed pressure measurements were made in the intake and exhaust runners, by Kistler piezoresistive absolute sensors: Type 4045A5 and water-cooled Kistler Type 4049A10S, respectively.

Temperatures were measured with K-type thermocouples. Gas and

Table 1

ASTM measured properties for the market Diesel fuel and surrogate fuel CN50_TSI31.

Fuel Property	Units	ASTM Procedure	Market Diesel Fuel	Surrogate CN50_TSI31
Derived Cetane Number		D6890	50.9	50.1
Smoke Point	mm	D1322	19.0	18.8
Threshold Soot Index			34	31
Net Heating Value	MJ/kg	D240N	43.004	42.857
Density at 15 °C	g/ml	D4052	0.849	0.831
Kinematic Viscosity at 40 °C	cSt	D445	3.06	2.41
Surface Tension	N/m	D3825	0.0312	0.0273
T ₁₀	°C	D86	226.8	220.6
T ₅₀	°C	D86	280.7	245.2
T ₉₀	°C	D86	311.7	272.4
Alkane Hydrocarbons	%v/v	D1319	76.0	82.7
Alkene Hydrocarbons	%v/v	D1319	7.5	4.9
Aromatic Hydrocarbons	%v/v	D1319	16.5	12.4
Total Aromatics	%m/m	D5186	16.4	16.4
H/C Molar Ratio	molR		1.85	1.87
Average Molecular Weight	g/mol		203	185
Stoichiometric A/F Ratio			14.58	14.60

Table 2
Single-cylinder engine characteristics and geometries.

Parameter	Units	Value
Compression Ratio		16.0
Cylinder Displacement	liter	0.4
Bore	mm	79.7
Stroke	mm	80.1
Combustion Chamber Bowl		Re-entrant
Fuel Injector		Solenoid
Number of Nozzle Holes		8
Nozzle Diameter	mm	0.116
Nozzle Flow Number	cc/30 s	340
Nozzle Included Angle	degrees	155

fluid temperatures (air, EGR, oil, and coolant) were measured by positioning the thermocouple end tip in the center of the flow stream, while surface thermocouples were welded throughout the intake and exhaust system to monitor and control surface temperatures.

3.2.4. Emission measurements

Gaseous emissions consisting of exhaust CO₂, CO, HC, NOx and O₂ and intake CO₂ were measured with a dual sample line Horiba MEXA D7500EGR emission bench. All sample lines were heated and the NOx and HC analyzers were contained in separately heated ovens. The emission bench was modified for high-pressure intake CO₂ sampling. The bench featured two exhaust sample lines with two complete sets of gas analyzers. Exhaust samples were taken from two locations and the measurements were compared to ensure data accuracy and quality. An additional quality check was made by routinely sampling from pre-mixed gas cylinders of known concentrations.

No measurable smoke was produced in this LTC operation mode, so no opacity results can be reported. Exhaust particle number density and size distribution were characterized with a Cambustion DMS500 fast particle analyser. Exhaust particle data were post-processed with proprietary Cambustion software. Data summaries included statistics that described the particle distribution such as total particle number concentration and particle geometric mean diameter. Particle spectral analysis were performed on the discrete mode, accumulation mode and nucleation mode.

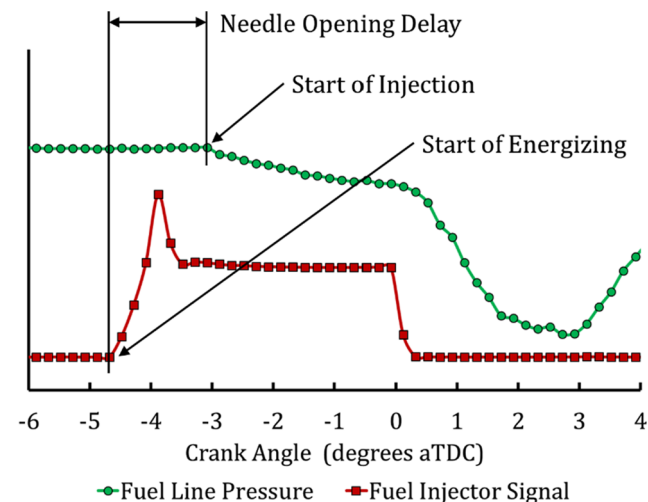


Fig. 2. Fuel injection events based on fuel line pressure and injector current.

3.3. Operating conditions

To evaluate the fuels under PPCI and LTC combustion conditions, a moderate engine speed of 1500 r/min and light engine load corresponding to 3 bar IMEP was used. Engine load was maintained by adjusting the fuel injection quantity at each test point. Some details of this operating condition are summarized in Table 3. The combination of moderate engine speed and relatively small quantities of injected fuel enabled a broad range of fuel-air mixing prior to ignition. The resulting matrix contained 24 test points for each fuel.

A single-injection strategy was selected to simplify the injection and combustion process and to focus on differences that result from the fuel properties. All tests were run at 50 °C intake temperature and the swirl ratio maintained at 2.9. The intake pressure was set based on the engine speed and load. The pressure differential between the intake and exhaust was held constant, which does not reproduce exactly a turbocharged engine with changing EGR rates. However, maintaining a constant pressure provides meaningful results and is very pragmatic for running the single-cylinder engine tests.

Two engine calibration parameters that have significant effects on combustion and emissions from PPCI and LTC are EGR dilution and

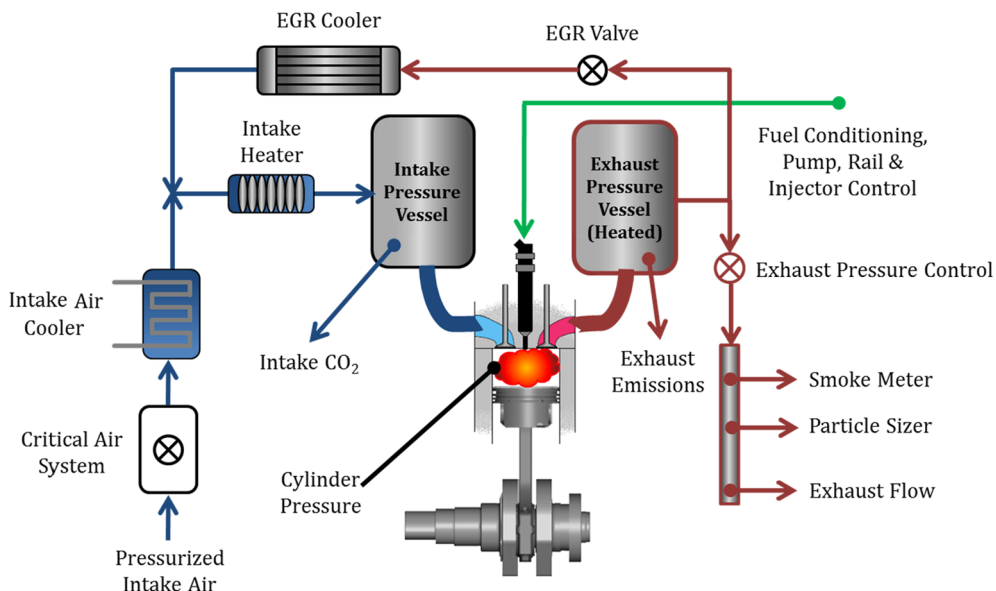


Fig. 1. Schematic of the single-cylinder engine test facility.

Table 3

Single-cylinder engine operating conditions to achieve PPCI and LTC conditions.

Parameter	Units	Value
Engine Speed	r/min	1500
Engine IMEP	bar	3
Fuel Injection Pressure	bar	550
Fuel Injection Strategy		Single
Injection Duration	ms	0.505–0.546
Intake Pressure	kPaA	102
Exhaust Pressure	kPaA	106
Intake Temperature	°C	50
Swirl Ratio		2.9
EGR Levels	%	0, 20, 40, 50, 55, 60
CA50 Timings	CAD aTDC	6, 9, 12, 15

combustion phasing as represented by the crank-angle of 50% mass burned (CA50). Therefore, a test matrix was developed based on adapting the start of energizing (SOE) depending on the EGR rate and for attaining the target values of CA50, while holding the other operating conditions constant.

The EGR sweep started at 0% which achieved PPCI combustion but did not obtain LTC due to high combustion temperatures. At EGR levels greater than 50%, combustion transitioned into the LTC regime. Therefore, EGR levels greater than 50% were more closely spaced in order to better characterize combustion, emissions and particles in the LTC regime. The EGR sweep ended at 60% EGR. The EGR rate was calculated by using the values of CO₂ concentration in the intake, the exhaust and the atmosphere by the following formula:

$$EGR(\%) = \frac{CO_{2intake} - CO_{2atmosphere}}{CO_{2exhaust} - CO_{2atmosphere}} \times 100$$

The needle opening delay, as defined in Fig. 2, was calculated for each test point. For the market Diesel fuel, the needle opening delay was determined to be essentially constant at 1.6 CAD throughout the EGR and CA50 sweeps. An unchanging opening delay was an expected result since engine speed and injection pressure were held constant throughout the tests. The needle opening delay for the surrogate fuel was also found to be effectively constant at 1.6 CAD. It was important for the surrogate fuel to match the opening delay of the market Diesel fuel thus demonstrating that differences in the physical properties of the fuel did not impact the response time of the injector.

As mentioned above, at each EGR level, the combustion phasing sweep was conducted at CA50 values of 6, 9, 12 and 15 CAD aTDC by adjusting the SOE at each test point. The resulting SOI and calculated bulk gas temperature (from cylinder pressure and ideal gas law) for the EGR sweeps are shown in Fig. 3(a). At the start of the EGR sweep, the injection SOI advance was about –3 CAD aTDC. From 0% to 40% EGR

the SOI required a moderate increase of 2.5 degrees in the advance to maintain combustion phasing. However, from 40% to 60% EGR the SOI required more than 7 degrees of additional advance to maintain CA50 at 9 CAD aTDC. Fig. 3(b) shows the resulting SOI and bulk gas temperature for changing the CA50 at a constant EGR level of 40%.

It is important to note that throughout the EGR and CA50 sweeps, the market Diesel fuel and surrogate fuel required similar injection SOI advance to control the combustion phasing. The average difference in injection SOI was 0.7 CAD (the crankshaft encoder resolution was 0.2 CAD). With the injector needle opening delay, the SOI advance, and the bulk gas temperature replicated, it can be concluded that the market Diesel fuel and surrogate fuel were injected into essentially the same in-cylinder conditions namely, temperature, pressure, density, mixture motion, and piston position. This is already an important finding that would tend to eliminate the in-cylinder conditions at the time of injection as a cause for combustion or emission differences observed between the market Diesel fuel and surrogate fuel.

4. Combustion results

PPCI smokeless combustion was achieved at all of the test conditions. The low engine speed coupled with a small fuel injected quantity and relatively low in-cylinder pressure and temperature provided sufficient mixing time for combustion to occur at low local equivalence ratios that avoided the soot formation due to the high equivalence ratio and high temperature conditions. Exhaust soot could not be detected with the Smoke Meter or the Opacimeter. However, exhaust particles were detected and characterized with the DMS500 particle sizer, as explained in Section 3.2.4.

Low Temperature Combustion was achievable only at EGR levels equal to or greater than 50%. This was deduced from the very low NOx emissions which indicated that the local combustion temperatures avoided also the NOx formation conditions occurring at low equivalence ratio and high temperature.

The combustion analysis began by studying the cylinder pressure measurements and the resulting heat release profiles at the two extreme cases of 0% EGR and 60% EGR. For both tests the combustion phasing was set at CA50 = 9 CAD aTDC which was the optimal combustion phasing for efficiency. Curves of in-cylinder pressure and heat release rate are plotted in Fig. 4, comparing the engine operating with the market Diesel fuel and with the surrogate fuel. For brevity, the net apparent heat release rate is referred to as heat release rate in this article.

The cylinder pressure shows significant differences between 0% EGR and 60% EGR. Early during the compression stroke, cylinder pressures were very similar for both EGR levels. Closer to TDC, the compression pressure at 60% EGR was less than at 0% EGR. This discrepancy in cylinder pressure occurred between –10 CAD and 0 CAD

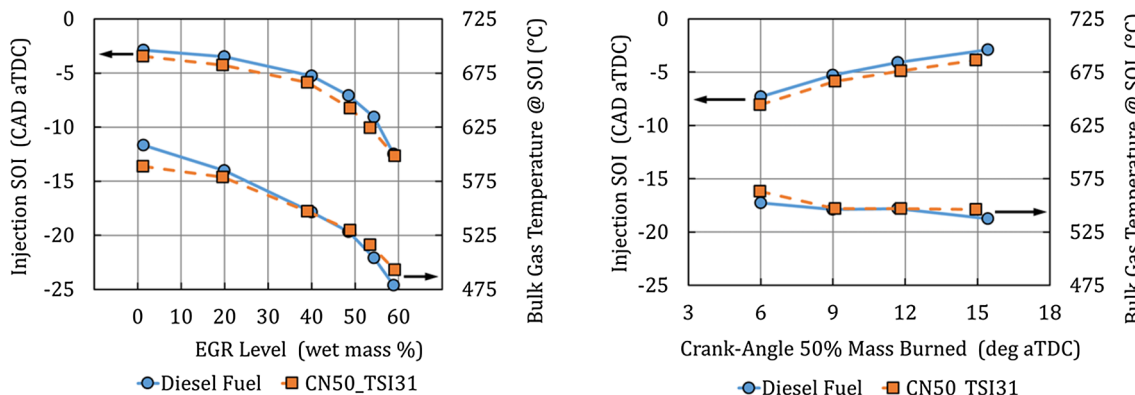


Fig. 3. Injection SOI and calculated Bulk Gas Temperature: (a): CA50 = 9 degrees aTDC as EGR level was increased from 0% to 60% (left) (b): CA50 = 6, 9, 12 and 15 degrees aTDC with 40% EGR.

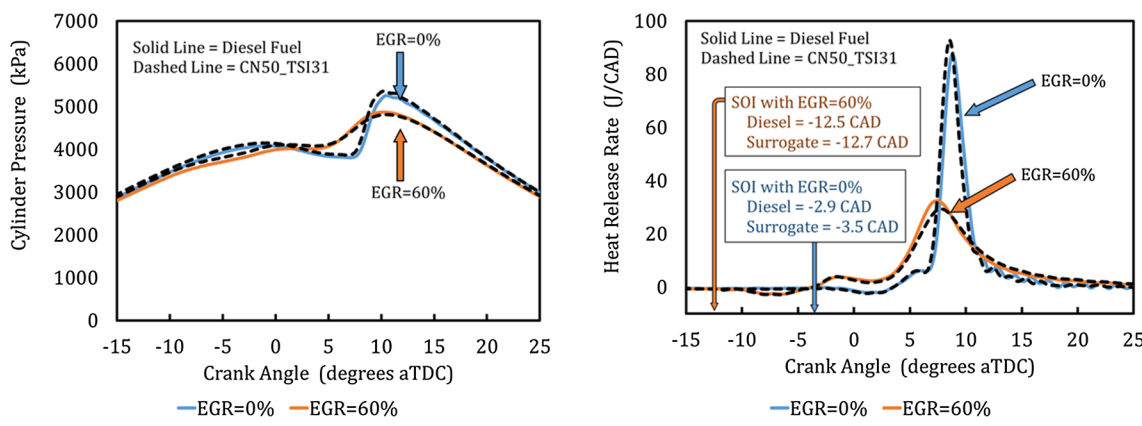


Fig. 4. In-cylinder pressure and heat release rate with 0% EGR and with 60% EGR. Injection SOI adjusted to maintain CA50 = 9 CAD aTDC for all tests.

at TDC and was believed to be the result of fuel vaporization. For the market Diesel fuel, at 60% EGR, the injection SOI was -12.5 CAD aTDC whereas the SOI was -2.9 CAD aTDC for 0% EGR.

Compared to 0% EGR, the 60% EGR condition resulted in lower cylinder pressure rise rates and lower peak cylinder pressures during combustion. Very good agreement was observed between the market Diesel fuel and the surrogate fuel. As a result of maintaining the CA50 at 9 CAD aTDC, the crank-angle of the peak cylinder pressures for 0% and 60% EGR were in close agreement for all tests (10.2 ± 0.1 CAD aTDC). For 0% EGR, the market Diesel fuel had a peak pressure of 5409 kPa while the surrogate peak pressure was 5387 kPa (a difference of less than 0.5%).

The same Fig. 4 (right) shows the comparison of the heat release rates, for both fuels, at 0% EGR and at 60% EGR. Again, the combustion phasing was held constant with CA50 = 9 CAD aTDC.

The 0% EGR condition had a clearly defined but relatively short duration of the low-temperature heat release period (LTHR) – between 0 and 7 CAD aTDC – followed by very rapid premixed combustion that reached a peak heat release rate around 95 J/CAD. The combustion duration from 10% to 90% mass burned was 4.3 CAD for the market Diesel fuel and 4.5 CAD for the surrogate fuel. At 60% EGR, the LTHR was greatly extended followed by a slower, longer duration premixed combustion. The duration of the 10–90% mass burn increased to 13.6 CAD for the market Diesel fuel and 13.2 CAD for the surrogate fuel. At both extreme operating conditions, the heat release rates from the market Diesel fuel were reasonably well-matched by the surrogate fuel.

The effects of combustion phasing on the cylinder pressure (Fig. 5 left) were investigated at constant EGR equal to 40% and changing SOI for achieving a sweep in CA50 from 6 CAD aTDC (advanced phasing) to 15 CAD aTDC (retarded phasing). As CA50 was retarded the ignition and peak cylinder pressure moved later into the expansion stroke which

significantly reduced the peak cylinder pressure and cylinder pressure rise rate. The data shows that during the combustion phasing sweep the cylinder pressure histories for the surrogate and market Diesel fuels were in very close agreement, with relative differences in the range of 1%.

Fig. 5 (right) also shows the same results in terms of heat release rate data and illustrates that as the CA50 was retarded from 6 to 15 CAD aTDC, the duration of the LTHR was extended, the ignition moved further into the expansion stroke, the peak heat release rate was reduced and moved further into the expansion stroke and the overall combustion duration was increased. In particular, the peak heat release rates were reduced by more than 50%. In general, the surrogate fuel replicated the heat release rates from the market Diesel fuel.

4.1. Low temperature heat release (LTHR)

Details of the LTHR at 0% EGR and 60% EGR with CA50 = 9 CAD aTDC are shown in Fig. 6. Data from the market Diesel fuel are shown with solid lines and the surrogate fuel data are shown with dashed lines. The y-axis and x-axis scales are expanded to focus on the LTHR regime.

For both EGR levels, the surrogate fuel followed the evaporation characteristics of the market Diesel fuel. For the 60% EGR condition, the advanced SOI placed the fuel evaporation period between -10 and -6 CAD aTDC. Whereas, less SOI advance was required for 0% EGR which positioned the evaporation period between -2 and 2 CAD aTDC.

The data in Fig. 6 show that the duration of the LTHR was significantly shorter for 0% EGR than for 60% EGR and the characteristic profiles were also considerably different. For both EGR levels, the surrogate fuel closely followed the heat-release attributes of the market Diesel fuel.

Two metrics were computed from the heat-release rate data to

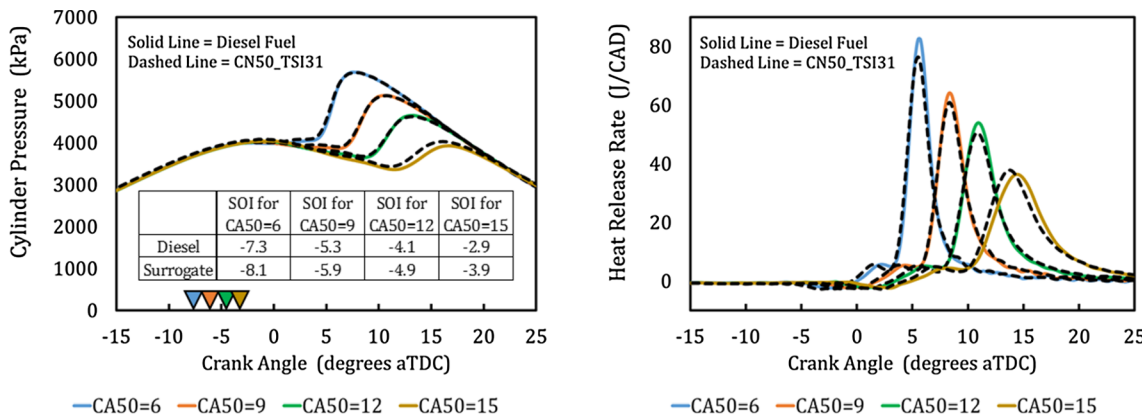


Fig. 5. Cylinder pressure and heat release rates for CA50 sweeps with 40% EGR.

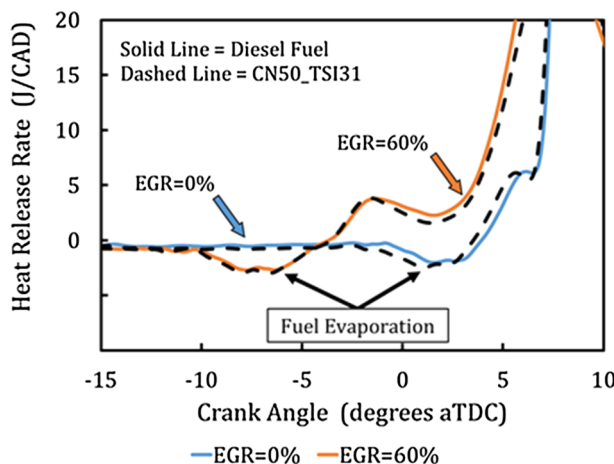


Fig. 6. Low temperature heat release with 0% EGR and 60% EGR. Injection SOI adjusted to maintain CA50 = 9 CAD aTDC.

comprehend the effects of EGR and compare the surrogate and market Diesel fuels. The first metric was the duration of the LTHR. The second metric was the total amount of heat released over the duration of the LTHR. The method used to determine the start and end of the low temperature heat release (LTHR) is illustrated in Fig. 7 and described herein. The start of the LTHR was defined as the local minimum of the region where the fuel evaporation transitioned to LTHR. The crank-angle location for the start of LTHR was detected by measuring the slope of the heat release rate profile. LTHR started when the slope transitioned from negative, or zero, to positive values. The end of the LTHR was defined as the local minimum of the region where LTHR transitioned to the high-temperature heat release regime. The crank-angle location for the end of LTHR was detected by measuring the slope of the heat release rate profile. LTHR ended when the slope transitioned from negative, or zero, to positive values. The total amount of heat released during the LTHR period was calculated by integrating the heat released from the start to the end of the LTHR period. Error bands for the LTHR calculations were determined by computing the difference in the LTHR with the start and end location varied by 0.2 CAD. The results were averaged and the error bands were set at 0.4 CAD for the duration and 0.5 J for the total amount of heat released.

The results in Fig. 8 show the effects of EGR on the total amount of heat release over the LTHR period and duration of the LTHR period. As EGR was increased from 0% to 50%, the duration of the LTHR increased from about 4 CAD to 6 CAD and the total amount of heat released rose from about 9 J to around 12 J. An interesting observation is the apparent transition that occurred around 50% EGR. As EGR was increased from 50% to 60%, the total amount of heat release dropped from about 12 J to about 9 J and the duration of the LTHR increased from 6 CAD to 8 CAD. It is not clear if the observations are the result of over-mixing that stems from the increased LTHR duration, the reduction in oxygen concentration, or a combination of factors. Comparing the fuels, the data shows the surrogate fuel essentially matched the duration of LTHR from the market Diesel fuel. Good agreement between the two fuels was also obtained for the total amount of heat release over the LTHR period with the error bars overlapping at all conditions except for 60% EGR. Both fuels exhibited the apparent transition in LTHR around 50% EGR.

4.2. Ignition delay

The impact of EGR on the ignition delay is shown in the left upper plot of Fig. 9. During the EGR sweep the combustion phasing was maintained at CA50 = 9 CAD aTDC. At 0% EGR the ignition delay was approximately 9 CAD and increased to about 14 CAD at 60% EGR. The test results show the ignition delay times for the market Diesel fuel and surrogate fuels were in good agreement. The average difference in

ignition delay was 0.5 CAD and the maximum observed difference was 0.9 CAD.

The right upper plots in Fig. 9 show the effects of combustion phasing on ignition delay at 40% EGR. Retarding the CA50 from 6 to 15 CAD aTDC increased the ignition delay by approximately 2 CAD. The test data show that the market Diesel and surrogate fuels followed the same trend. The average difference in ignition delay was 0.5 CAD and the maximum observed difference was 0.6 CAD.

During the course of the EGR and CA50 sweeps, the market Diesel and surrogate fuel had similar ignition delay times. The data shown in Fig. 8 suggested that fuels also had very similar low-temperature heat release during the ignition delay. With the SOE, SOI, ignition delay time, and low-temperature heat release well-matched for both fuels, it was concluded that nearly the same in-cylinder conditions such as, temperature, pressure, density, mixture motion, and piston position were present at the onset of ignition. This was an important finding that would tend to eliminate the in-cylinder conditions at the time of ignition as a cause for combustion or emission differences observed between the market Diesel and surrogate fuel.

4.3. Peak heat release rate

The mid plots in Fig. 9 show the effects on the values of the peak heat release rates for both fuels. As EGR was increased and injection SOE was advanced to maintain CA50 = 9, the peak heat release rate dropped considerably. At 60% EGR the peak heat release rate fell to about one third from the case 0% EGR. The effects of combustion phasing on the peak heat release rate with 40% EGR show that retarding from CA50 = 6 to 15 CAD aTDC reduced the peak heat release rate by approximately 50%.

In both sweeps, the surrogate fuel closely followed the peak heat release rates of the market Diesel fuel.

4.4. 10–90% burn duration

Finally, the lower plots in Fig. 9 present the effects of EGR and CA50 on the 10–90% burn duration. During the EGR sweep and constant CA50 = 9 CAD, the increase in EGR from 0% to 40% marginally increased the burn duration (a total increase of about 1 CAD). As EGR was increased from 40% to 60%, the burn duration markedly increased by about 8 CAD. The effects of retarding the combustion phasing at constant 40% EGR allow to quantify the trends already observed in Fig. 5, by an increase in the burn duration of around 5 CAD.

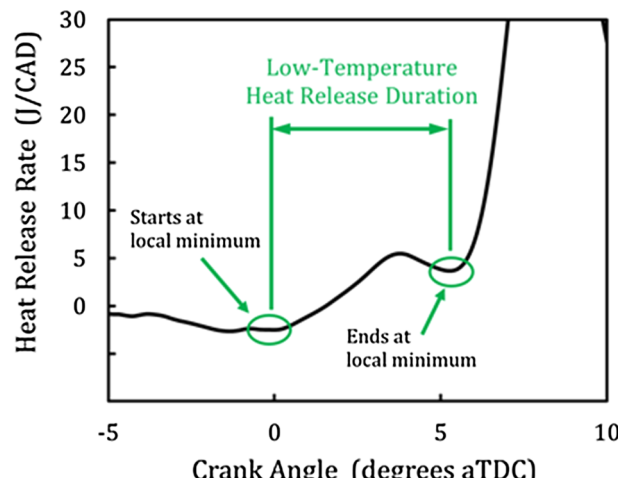


Fig. 7. Heat release rate plot showing the method to determine the start, end, and duration of the low temperature heat release.

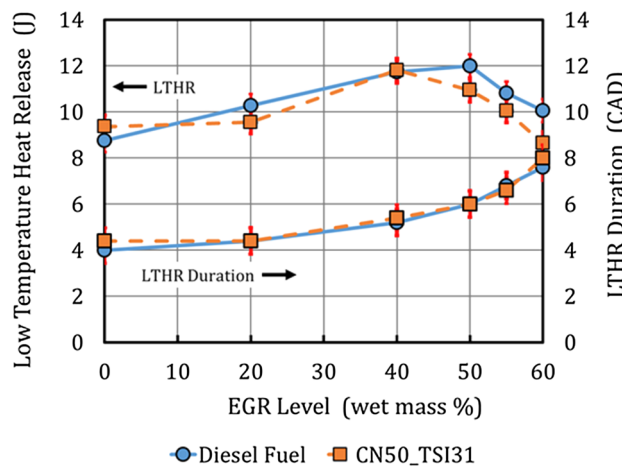


Fig. 8. EGR effects on total amount of heat released over the LTHR period and on the duration of the LTHR.

Throughout the EGR and CA50 sweeps, the 10–90% burn durations from the market Diesel fuel were well-matched by the surrogate fuel. The average difference in the burn duration was smaller than 1 CAD and the maximum observed difference was smaller than 2 CAD.

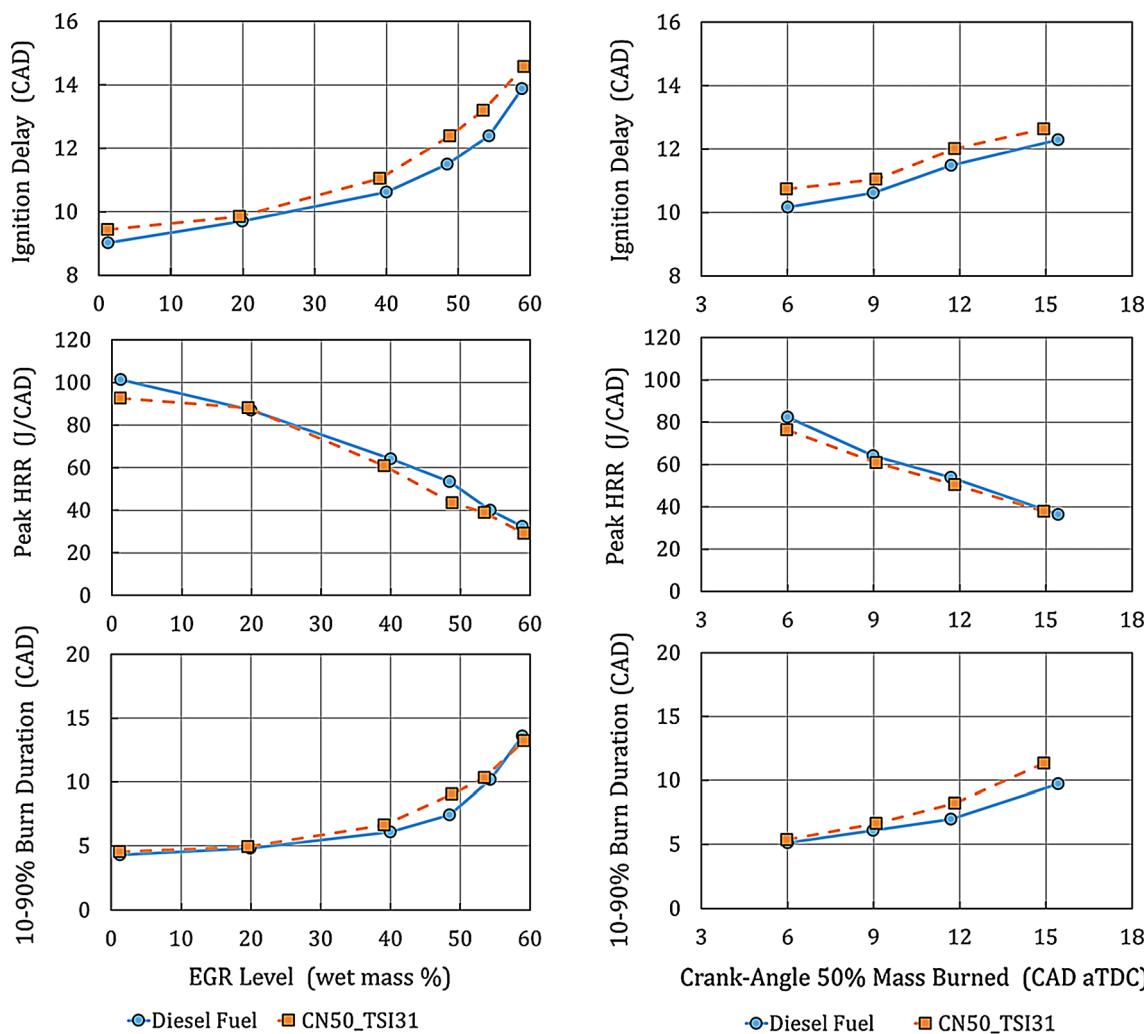


Fig. 9. Combustion results from EGR and CA50 sweeps for the Diesel and surrogate fuels. The EGR sweeps were run at CA50 = 9 CAD aTDC and the CA50 sweeps were run at 40% EGR.

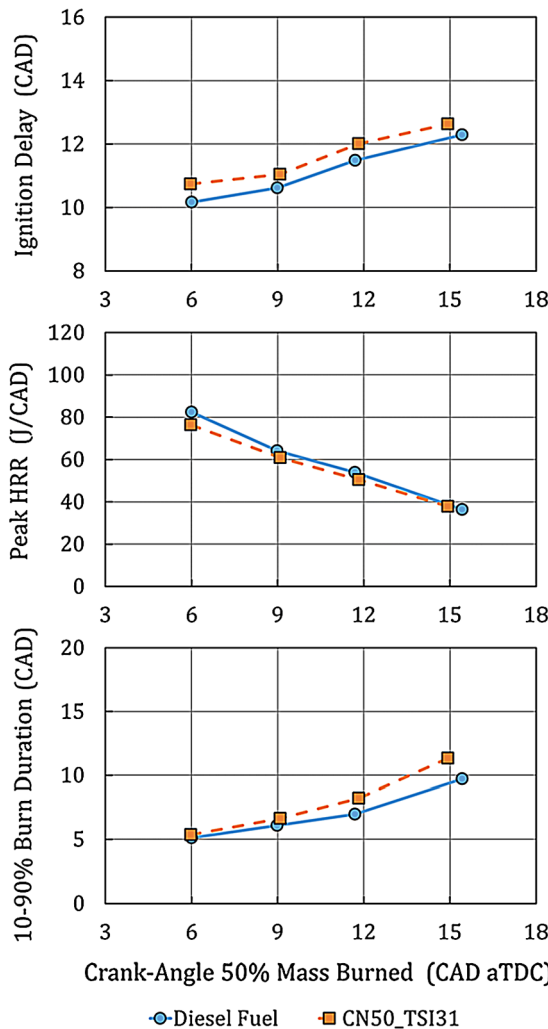
5. Combustion efficiency and gaseous emissions

Researchers have reported about the impact of PCCI and LTC on combustion, efficiency and emissions. For example, Jacobs et al. developed a premixed LTC combustion strategy that sharply lowered particulate and NOx emission at the expense of increased fuel consumption, HC and CO emissions [28]. One step further to assess the capability of the surrogate fuel in representing the market Diesel fuel with accuracy is to compare the combustion efficiency and pollutant emissions under the PCCI and LTC conditions. As described in Section 4, both fuels exhibited a very similar global heat release process, however, differences in local in-cylinder conditions that affect the formation of pollutants can still appear. The cause can be small differences in fuel physical properties such as density, viscosity and distillation temperatures that can affect the mixture preparation during the ignition delay period, liquid penetration, fuel vapor distribution and the local fuel-air mixture during combustion.

Fig. 10 shows results for the combustion efficiency and gaseous emissions from the EGR and CA50 sweeps. The emissions are presented on an Emission Index (EI) basis with units of g/kg-fuel.

5.1. Combustion efficiency

As one would expect, Fig. 10 shows the PCCI and LTC combustion has an adverse effect on combustion efficiency. On average, increasing



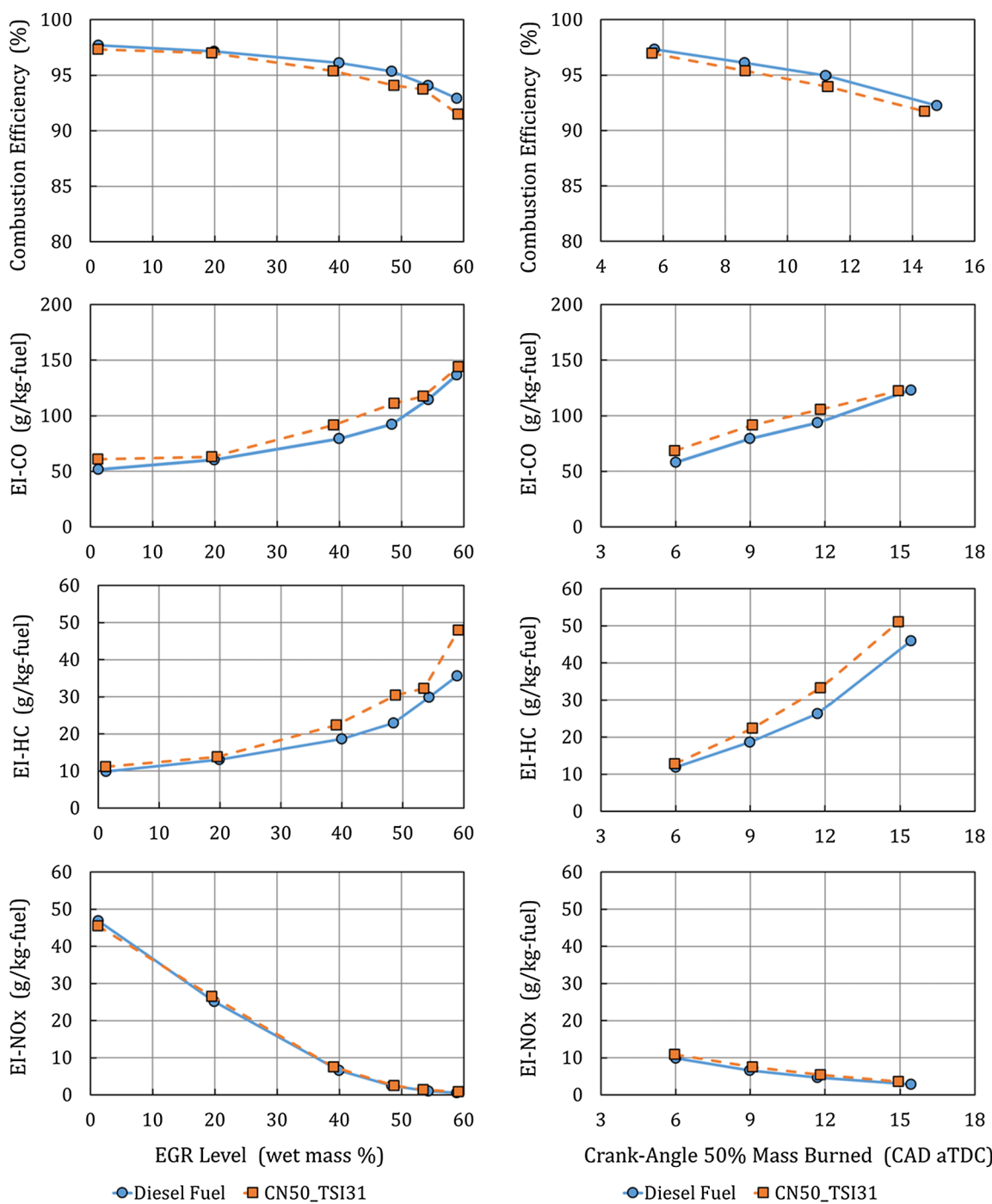


Fig. 10. Combustion efficiency and gaseous emissions results for Diesel and surrogate fuels: – left: EGR sweep from 0% to 60% at constant CA50 = 9 CAD aTDC – right: CA50 sweep at constant 40% EGR.

the EGR from 0% to 60% significantly lowered the combustion efficiency from 97% to 92%. At the 40% EGR rate, retarding the combustion phasing from CA50 = 6 to 15 also decreased the combustion efficiency from approximately 97% to 92%. The surrogate fuel followed the trends of the market Diesel fuel with an overall average combustion efficiency difference of 0.7% and a maximum difference of 1.4% at the 60% EGR condition.

5.2. CO

For these operating conditions, low combustion temperatures and more time for mixing resulted in less CO oxidation and higher engine-out CO emissions. As EGR increased from 0% to 60%, combustion transitioned into the LTC regime and the CO emissions increased to a final value of about 150 g/kg-fuel. Moreover, and contrary to the small

effect observed at other higher-load operating conditions [25] at 40% EGR, the retarding of the combustion phasing from CA50 = 6 to 15 essentially doubles the EI-CO to a final value of 120 g/kg-fuel.

Even at these elevated CO levels the surrogate fuel replicated the emissions from the market Diesel fuel. The trends were consistent and the EI-CO difference averaged about 9%. This result suggests that the overall mechanisms leading to incomplete CO oxidation to CO₂ were not significantly different between the two fuels.

5.3. HC

The exhaust HC emissions for the EGR sweep in Fig. 10 range from 10 to about 40 g/kg-fuel. Introducing EGR up to 60% has the plausible effect of reducing local oxygen concentrations and temperature which hinders complete hydrocarbon oxidation.

For the combustion phasing sweep, retarding the phasing increased the mixing time and lowered combustion temperatures which produces an increase in the HC emissions similar to that of CO.

Turning the attention to a comparison of the market Diesel and surrogate fuels, the average EI-HC difference between the fuels was about 5%. The data shows at EGR levels less than 60%, the two fuels had very good agreement. For this data, the average difference in EI-HC was only 3.6 g/kg-fuel. At 60% EGR, the surrogate fuel resulted in somewhat higher HCs than the market Diesel fuel. It's not clear if the surrogate fuel properties resulted in the higher HC emissions or if the reproducibility of operating conditions resulted in the increased HC emissions. Overall, the surrogate fuel adequately replicated the HC emission results obtained with the market Diesel fuel.

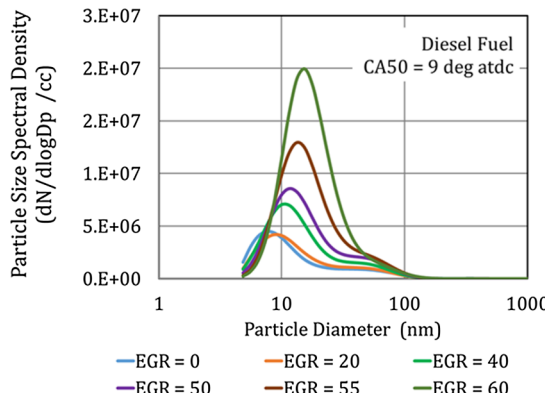
5.4. NOx

The same comparison as above in terms of NOx shows the expected trends. On one hand, a sharp reduction produced by the increase in EGR up to the detectability levels of the emission analyzer (EI-NOx = 0.5 g/kg-fuel). The retardation in the combustion phasing also achieves a reduction in NOx, as expected.

The test results from the EGR and combustion phasing sweeps show the market Diesel fuel and CN50_TSI31 fuels produced essentially the same NOx emissions.

6. Smoke and particle emissions

As shown earlier in Table 1, the surrogate fuel CN50_TSI31 was formulated to precisely match the TSI value of the market Diesel fuel, and the smoke point was replicated, too. This section examines the hypothesis that the threshold soot index may be used to formulate a surrogate fuel that will produce the same exhaust smoke and particles as a full-range petroleum Diesel fuel.



6.1. Exhaust smoke

The current operating condition was developed to provide PPCI combustion that transitioned into low temperature combustion with the addition of EGR. The in-cylinder conditions provided sufficient fuel-air mixing that resulted in smoke-free combustion at all of the test points. Therefore, no comparative results can be shown in terms of smoke opacity.

6.2. Exhaust particles

The use of the Cambustion DMS500 allowed to determine the particle number (N), particle diameter (D_p), and the particle expression dN/dlogD_p. Plotting the particle expression dN/dlogD_p as a function of D_p generates a graph known as the particle size distribution. The particle distributions were characterized by two modes: nucleation and accumulation. The nucleation mode particles were smaller than 30 nm and considered to be volatile material. Accumulation mode particles were considered to be solid and larger than 30 nm. The particle number concentration (N/cc) was calculated from the integrated particle size distributions for each mode. That is to say, the nucleation and accumulation mode particles were integrated separately. The particle count median diameter (CMD) was the particle diameter at the peak of each mode.

Fig. 11 shows the particle size distributions from an EGR sweep with the CA50 = 9 CAD aTDC while the engine was operating on the market Diesel fuel. In contrast to the particle size distributions for conventional Diesel combustion, the particles from PPCI (0% EGR) and LTC (60% EGR) were primarily nucleation mode particles with trace amounts of accumulation mode particles. Small amounts of EGR, for example 20%, had little impact on the particle size distribution. Greater amounts of EGR steadily increased the number of nucleation mode particles. The peak of the distribution also shifted to larger diameters.

The effect of combustion phasing on the particle size distribution is illustrated in Fig. 11. The CA50 sweep was conducted at 60% EGR which was considered to be a low-temperature combustion condition. The results show that retarded combustion phasing had a substantial impact on the particle size distribution. The number of nucleation mode particles increased and the distribution shifted to larger diameters.

Given the general understanding of the effects of EGR and combustion phasing on the particle size distributions for PPCI and low temperature combustion, the next step was to compare the exhaust particles from the market Diesel fuel with the particles from the surrogate fuel. This was accomplished by comparing the particle number concentrations (N/cc) and count median diameters (CMD) in lieu of generating numerous overlays of particle size distributions.

The effects of EGR on the particle number concentration, separating nucleation and accumulation modes is given in Fig. 12 (left). The data

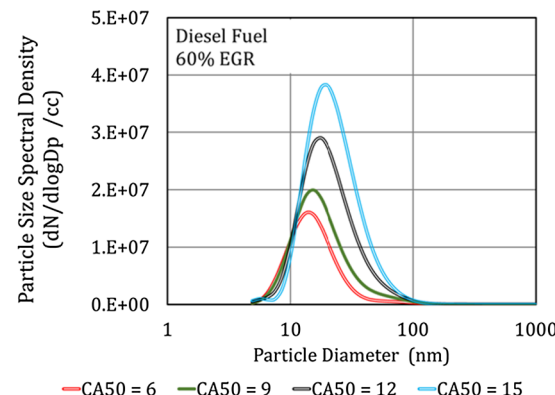


Fig. 11. Particle size spectral density for the market Diesel fuel:- left: EGR sweep from 0% to 60% at constant CA50 = 9 CAD aTDC- right: CA50 sweep at constant 60% EGR.

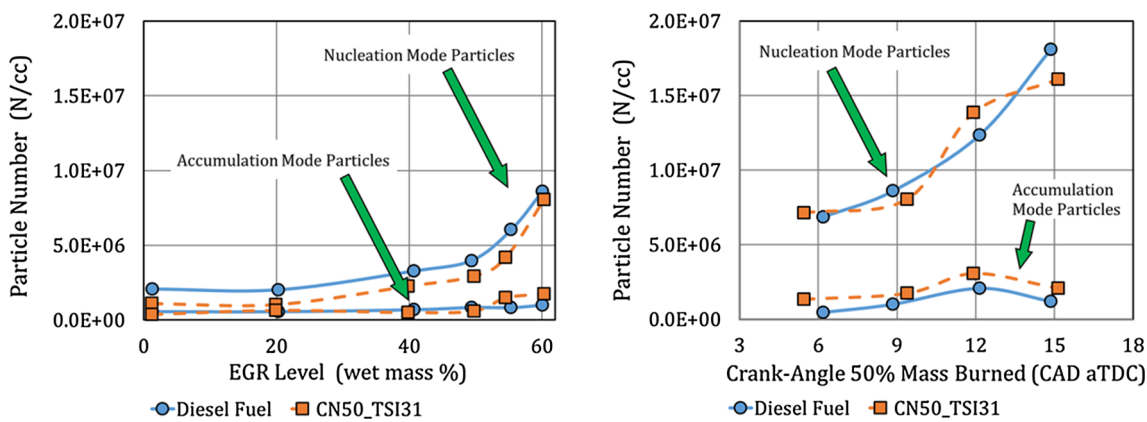


Fig. 12. Particle number concentrations for Diesel and surrogate fuels:- left: EGR sweep from 0% to 60% at constant CA50 = 9 CAD aTDC- right: CA50 sweep at constant 60% EGR.

were acquired with the combustion phasing set at CA50 = 9 CAD aTDC.

The data in Fig. 12 shows accumulation mode number concentrations for the market Diesel and surrogate fuels were in relatively good agreement. Throughout the EGR sweep the accumulation mode particle number concentrations were very low and not significantly affected by EGR.

The nucleation mode particle number concentration steadily rose as EGR was increased from 0% to 50%. Above 50% EGR, the nucleation particle number concentration increased at a faster rate. The EGR effects were similar to the trends for CO and HC emissions (Fig. 10). The market Diesel and surrogate fuels followed the same trends with increasing EGR. However, the market Diesel fuel exhibited higher nucleation particle concentration throughout the EGR sweep.

Fig. 12 (right) also shows the effects of combustion phasing on the particle number concentration. The data were acquired with 60% EGR for ensuring a low temperature combustion condition. At 60% EGR, the nucleation particle concentration had increased to about 8.3E + 06 N/cc. A combustion phasing sweep at this condition should provide a rigorous comparison of the fuel particle concentrations.

The accumulation particle concentrations slightly increased as combustion phasing was retarded from CA50 = 6 to 12 CAD aTDC then reduced to lower concentrations at the most retarded phasing of CA50 = 15 CAD aTDC. The market Diesel and surrogate fuels followed the same trends. On average, the accumulation mode particle number concentration from the surrogate fuel was 54% greater than the market Diesel fuel. The nucleation particle concentrations increased by nearly 2.5 times as the combustion phasing was retarded. In general, the

nucleation particle concentrations from the market Diesel and surrogate fuels were in good agreement; although the surrogate fuel trend was not as smooth as the market Diesel fuel.

The particle count median diameter (CMD) results from the EGR sweeps are shown in Fig. 13. For both fuels, the nucleation particle CMD steadily increased with increasing EGR. The surrogate fuel closely replicated the nucleation particle CMD from the market Diesel fuel. For both fuels, an interesting trend occurred above 50% EGR namely, the accumulation particle CMD reduced to about the same value than the case with 0% EGR.

CMD results from the combustion phasing sweep at 60% EGR are given also in Fig. 13. As CA50 was retarded from 6 to 15 CAD aTDC, the nucleation particle CMD steadily increased. The accumulation particle CMD were essentially unchanged averaging 40 nm as the combustion phasing was retarded from CA50 = 6 to 12 CAD aTDC. The data show the accumulation particle CMD somewhat increased at the most retarded combustion phasing of CA50 = 15 CAD aTDC. The test results suggest that overall, the accumulation and nucleation particle CMD from the market Diesel fuel were well-matched by the surrogate fuel.

The test data shown in Figs. 12 and 13 indicate that the trends in particle number concentration and count median diameter produced by the market Diesel fuel were reproduced when the engine was operated on the surrogate fuel. This was a very important finding. The results suggest that for the PCCI and LTC combustion investigated herein, the surrogate fuel TSI value may be used as an objective to formulate relatively simple multi-component surrogate fuels that will replicate the particle number concentrations and count median diameters from very

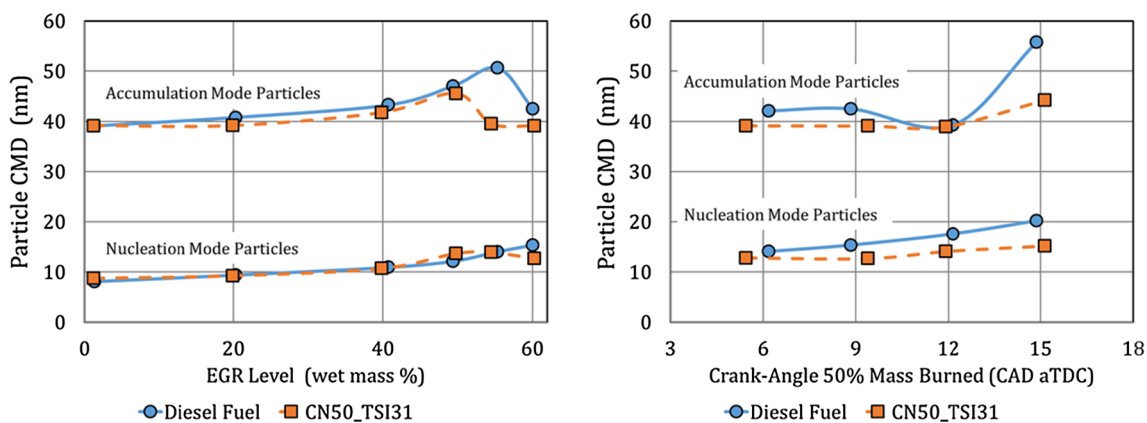


Fig. 13. Particle count median diameter (CMD) for Diesel and surrogate fuels:- left: EGR sweep from 0% to 60% at constant CA50 = 9 CAD aTDC- right: CA50 sweep at constant 60% EGR.

complex full-range petroleum Diesel fuels. A similar finding was obtained from previous work that investigated the surrogate fuel under conventional Diesel combustion conditions at 1500 r/min and 9 bar IMEP [25].

7. Summary and conclusions

Addressing the immediate need to apply fully-representative Diesel surrogate fuels to advance the understanding and development of future combustion systems, this work evaluated a market Diesel fuel and its corresponding surrogate fuel in a single-cylinder engine with contemporary fuel injection and combustion technology. In previous works, the surrogate fuel was formulated to closely match the physical, chemical and combustion properties of the market Diesel fuel [12,24] and experimentally evaluated under conventional Diesel combustion conditions [25]. This article extends the understanding and application of the surrogate by evaluating the fuel under partially-premixed and low temperature combustion regimes. With this objective, the engine was operated with sufficient in-cylinder fuel-air mixing to obtain PPCI combustion and high EGR levels to achieve both PPCI and LTC combustion. The surrogate fuel response to changes in the in-cylinder conditions were achieved by conducting EGR and CA50 sweeps.

For the PPCI and LTC regimes, it is essential that the surrogate closely reproduce the ignition delay, low temperature heat release and high temperature heat release characteristics of the market Diesel fuel. The engine test results clearly demonstrated that the combustion attributes of the market Diesel fuel were very closely matched by the four-component surrogate fuel. Additionally, the gaseous emissions and particle distributions were also closely matched by the surrogate fuel. These experimental results support the hypotheses that closely matching the physical, chemical and combustion properties of a market Diesel fuel can provide a practical and effective surrogate even though the particular hydrocarbon species that composes the surrogate may only be sparsely present, or absent, in the market Diesel fuel.

It is plausible to conclude that by matching density, viscosity, surface tension, and the distillation curve that the surrogate fuel matched the fuel spray, vapor formation and local equivalence ratios of the market Diesel fuel. By matching cetane number, TSI, and heating value, it is also possible to conclude that, prior to ignition, the surrogate fuel decomposed into essentially the same effective light, unsaturated hydrocarbons as the market Diesel fuel. Hence, the Diesel and surrogate fuels provided essentially the same in-cylinder conditions that resulted in the same ignition, combustion, gaseous emissions and exhaust particles for the PPCI and LTC conditions.

This investigation demonstrates that a simple four-component surrogate can match the combustion and emissions characteristics of a market Diesel fuel under PPCI and LTC regimes. Given these findings, further investigations of such surrogates are warranted including the development of detailed and reduced kinetic mechanisms for combustion simulation, experimental investigations of the reacting spray, engine testing over a broader range of operating conditions, and the evaluation of surrogates with varied cetane numbers and sooting tendencies.

Acknowledgements

The authors thank General Motors Global Research and Development for supporting this research. Additionally, the authors would like to thank Venkatesh Gopalakrishnan, Vicent Domenech-Llopis, Seunghwan Kuem and Richard Peterson for their insight and contributions to this work.

References

- [1] The Society of Motor Manufacturers and Traders. New Car CO₂ Report, 2018. <https://www.smmt.co.uk/wp-content/uploads/sites/2/SMMT-New-Car-Co2-Report-2018.pdf>.
- [2] US Drive. Advanced Combustion and Emission Control Roadmap, March 2018. https://www.energy.gov/sites/prod/files/2018/03/f49/ACE_TT_Roadmap_2018.pdf.
- [3] Hardy WL, Reitz RD. An experimental investigation of partially premixed combustion strategies using multiple injections in a heavy-duty Diesel engine. SAE technical paper 2006-01-0917.
- [4] Okude K, Mori K, Shiino S, Moriya T. Premixed compression ignition (PCI) combustion for simultaneous reduction of NO_x and soot in Diesel engine. SAE technical paper 2004-01-1907.
- [5] Takeda Y, Keiichi N, Keiichi N. Emission characteristics of premixed lean Diesel combustion with extremely early staged fuel injection. SAE technical paper 961163.
- [6] Anand K, Ra Y, Reitz R, Bunting B. Surrogate model development for fuels for advanced combustion engines. Energy Fuels 2011;25(4):1474–84. <https://doi.org/10.1021/ef101719a>.
- [7] Kalghatgi G, Hildingsson L, Harrison A, Johansson B. Surrogate fuels for premixed combustion in compression ignition engines. Int J Engine Res 2011;12(5):452–65. <https://doi.org/10.1177/1468087411409307>.
- [8] Pitz W, Mueller C. Recent progress in the development of Diesel surrogate fuels. Prog Energy Combust Sci 2011;37(3):330–50. <https://doi.org/10.1016/j.pecs.2010.06.004>.
- [9] Luo J, Yao M, Liu H, Yang B. Experimental and numerical study on suitable Diesel fuel surrogates in low temperature combustion conditions. Fuel 2012;97:621–9. <https://doi.org/10.1016/j.fuel.2012.02.057>.
- [10] Design Institute for Physical Properties. AIChE DIPPR Project 801 – Full Version, KNowledge Corporation, 2005; 2008–2012; 2015; 2016. <http://App.KnowleDGE.com/Hotlink/Toc/Id:Kpdipprf7/Dippr-Project-801-Full/Dippr-Project-801-Full;2016>.
- [11] Mueller CJ, Cannella WJ, Bays JT, Bruno TJ, Defabio K, Dettman HD, et al. Diesel surrogate fuels for engine testing and chemical-kinetic modeling: compositions and properties. Energy Fuels 2016;30:1445–61. <https://doi.org/10.1021/acs.energyfuels.5b02879>.
- [12] Szymkowicz P. Analytical and Experimental Investigation of Multi-Component Surrogate Diesel Fuels [Ph.D Thesis]. Universitat Politècnica de Valencia; 2017.
- [13] Lindstedt R, Maurice L. Detailed kinetic modelling of n-heptane combustion. Combust Sci Technol 1995;107(4–6):317–53. <https://doi.org/10.1080/00102209508907810>.
- [14] Curran H, Gaffuri P, Pitz W, Westbrook C. A comprehensive modeling study of n-heptane oxidation. Combust Flame 1998;114(1–2):149–77. [https://doi.org/10.1016/s0010-2180\(97\)00282-4](https://doi.org/10.1016/s0010-2180(97)00282-4).
- [15] Tao F, Reitz R, Foster D. Revisit of Diesel reference fuel (n-heptane) mechanism applied to multidimensional Diesel ignition and combustion simulations. Seventeenth international multidimensional engine modeling user's group meeting. 2007.
- [16] Desantes J, Lopez J, Garcia J, Pastor J. Evaporative Diesel spray modeling. Atom Sprays 2007;17(3):193–231. <https://doi.org/10.1615/atomizspr.v17.i3.10>.
- [17] Payri R, Salvador FJ, Gimeno J, Peraza JE. Experimental study of the injection conditions influence over n-dodecane and Diesel sprays with two ECN single-hole nozzles. Part II: reactive atmosphere. Energy Convers Manage 2016;126:1157–67. <https://doi.org/10.1016/j.enconman.2016.07.079>.
- [18] Pei Y, Mehl M, Liu W, Lu T, Pitz W, Som S. A multicomponent blend as a Diesel fuel surrogate for compression ignition engine applications. J Eng Gas Turbines Power 2015;137. <https://doi.org/10.1115/1.4030416>.
- [19] Westbrook C, Pitz W, Herbinet O, Curran H, Silke E. A comprehensive detailed chemical kinetic reaction mechanism for combustion of n-alkane hydrocarbons from n-octane to n-hexadecane. Combust Flame 2009;156(1):181–99. <https://doi.org/10.1016/j.combustflame.2008.07.014>.
- [20] ANSYS Model Fuel Library, ANSYS reaction design. San Diego; 2015.
- [21] Johnson R, Natelson R, Kurman M, Miller D, Cernansky N. The auto-ignition of JP-8, Jet A, and selected fuel components in a single cylinder engine. Western States Section of the Combustion Institute Fall Meeting, WSCI-05F-55; 2005.
- [22] Poon HM, Pang KM, Ng HK, Gan S, Schramm J. Development of multi-component Diesel surrogate fuel models – Part I: validation of reduced mechanisms of Diesel fuel constituents in 0-D kinetic simulations. Fuel 2016;180:433441. <https://doi.org/10.1016/j.fuel.2016.04.043>.
- [23] Poon HM, Pang KM, Ng HK, Gan S, Schramm J. Development of multi-component Diesel surrogate fuel models – part II: validation of the integrated mechanisms in 0-d kinetic and 2-D CFD spray combustion simulations. Fuel 2016;181:120–30. <https://doi.org/10.1016/j.fuel.2016.04.114>.
- [24] Szymkowicz P, Benajes J. Development of a Diesel surrogate fuel library. Fuel 2018;222:21–34. <https://doi.org/10.1016/j.fuel.2018.01.112>.
- [25] Szymkowicz P, Benajes J. Single-cylinder engine evaluation of a multi-component Diesel surrogate fuel as a part-load operating condition with conventional combustion. Fuel 2018;226:286–97. <https://doi.org/10.1016/j.fuel.2018.03.157>.
- [26] Kitamura T, Ito T, Senda J, Fujimoto H. Mechanism of smokeless Diesel combustion with oxygenated fuels based on the dependence of the equivalence ratio and temperature on soot particle formation. Int J Engine Res 2002;3(4):223–48. <https://doi.org/10.1243/146808702762230923>.
- [27] Benajes J, Molina S, Novella R, Amorim R. Study on low temperature combustion for light-duty diesel engines. Energy Fuels 2010;24(1):355–64. <https://doi.org/10.1021/ef900832c>.
- [28] Jacobs T, Bohac S, Assanis D, Szymkowicz P. Lean and rich premixed compression ignition combustion in a light-duty Diesel engine. SAE Technical Paper Series 2005. <https://doi.org/10.4271/2005-01-0166>.
- [29] Kolodziej C. Particulate matter emissions from premixed diesel low temperature combustion. Universitat Politècnica de Valencia; 2012. Ph.D.
- [30] Benajes J, García-Olivé J, Novella R, Kolodziej C. Increased particle emissions from

- early fuel injection timing Diesel low temperature combustion. Fuel 2018;94:184–90. <https://doi.org/10.1016/j.fuel.2011.09.014>.
- [31] Desantes J, Bermúdez V, García J, Fuentes E. Effects of current engine strategies on the exhaust aerosol particle size distribution from a Heavy-Duty Diesel Engine. *J Aerosol Sci* 2005;36(10):1251–76. <https://doi.org/10.1016/j.jaerosci.2005.01.002>.
- [32] Benajes J, López J, Novella R, García A. Advanced methodology for improving testing efficiency in a single-cylinder research Diesel engine. *Exp Tech* 2008;32(6):41–7. <https://doi.org/10.1111/j.1747-1567.2007.00296.x>.
- [33] Riazi M, Daubert T. Simplify property predictions No.3, p.115-116, & p.107-112 Hydrocarbon processing. U.S.A.: Gulf Publishing; 1980.
- [34] Calcote H, Manos D. Effect of molecular structure on incipient soot formation. *Combust Flame* 1983;49(1–3):289–304. [https://doi.org/10.1016/0010-2180\(83\)90172-4](https://doi.org/10.1016/0010-2180(83)90172-4).
- [35] Heywood J. Internal combustion engine fundamentals. 1st ed. New York: McGraw-Hill; 2000.
- [36] Gątowski J, Balles E, Chun K, Nelson F, Ekchian J, Heywood J. Heat release analysis of engine pressure data. SAE Technical Paper Series 1984. <https://doi.org/10.4271/841359>.
- [37] Lapuerta M, Armas O, Hernández J. Diagnosis of DI Diesel combustion from in-cylinder pressure signal by estimation of mean thermodynamic properties of the gas. *Appl Therm Eng* 1999;19(5):513–29. [https://doi.org/10.1016/s1359-4311\(98\)00075-1](https://doi.org/10.1016/s1359-4311(98)00075-1).
- [38] Payri F, Molina S, Martín J, Armas O. Influence of measurement errors and estimated parameters on combustion diagnosis. *Appl Therm Eng* 2006;26(2–3):226–36. <https://doi.org/10.1016/j.applthermaleng.2005.05.006>.
- [39] A&D Technology, CAS 4.0 Reference Manual, A&D Technology, Inc., First Edition, 2009.